REYNOLDS NUMBER EFFECTS FOR NON-CHANNELIZED NON-AXISYMMETRIC PARTICLE-DRIVEN GRAVITY CURRENTS

<u>S. Laizet</u>[*1], E.P. Francisco[2], L.F.R. Espath[2], C.A.S Moser[2], and J.H. Silvestrini[2]

[1]*Department of Aeronautics, Imperial College London, UK*
[2]*Faculdade de Engenharia, Pontificia Universidade Catlica do Rio Grande do Sul, Porto Alegre, Brasil*

<u>*Summary*</u> The purpose of this numerical work is to investigate the influence of the Reynolds number on the evolution of particle-laden gravity currents in a non-channelized non-axisymmetric lock-exchange configuration by means of high-fidelity simulations. Such configurations are largely understudied by comparison to more conventional channelized or axisymmetric lock-exchange configurations, despite the fact that most of gravity currents in nature originate from non-channelized non-axisymmetric configurations. It is found that the Reynolds number has a strong influence on the lobe-and-cleft structures at the head of the current and on the deposition patterns over the flat bed.

INTRODUCTION

Turbidity currents are particle-laden gravity-driven currents in which the gravitational driving force is supplied by a density excess associated with the suspension of particles. They exhibit a highly complex dynamic with the presence of the lobe-and-cleft patterns at the front of the head and a region of mixing with intense spanwise Kelvin-Helmholtz vortices. Understanding the physical mechanism associated with these currents as well as the correct prediction of their main features are of great importance for practical and theoretical purposes. They have been under scrutiny for a very long time with many experimental investigations and more recently with numerical investigations based on Direct Numerical Simulations. However, most of those investigations were performed in a channelized flow configuration for which the flow is constraint by the wall in the spanwise direction. Following our previous work on channelized turbidity currents [2], high-fidelity simulations are performed in a non-channelized non-axisymmetric configuration where the current can freely evolved in the streamwise direction as well as in the spanwise direction. In the present numerical investigations, the aim is to better understand the effect of the Reynolds number on the spatio-temporal evolution of a non-channelized non-axisymmetric gravity current. The focus will be on the lobe-and-cleft structures at the front of the current and on the deposition pattern at the bottom wall.

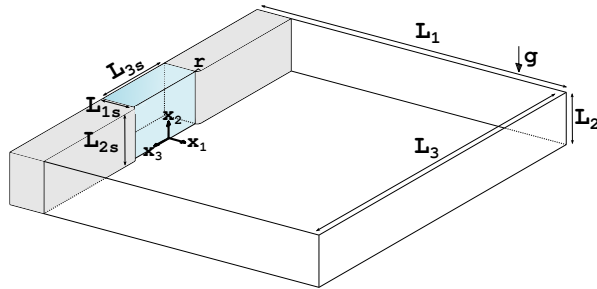## NUMERICAL METHODS AND FLOW CONFIGURATION

Figure 1: Schematic view of the flow configuration.

The fluid-particle mixture (in blue in Figure 1) is enclosed in a small portion of the domain $L_{1s} \times L_{2s} \times L_{3s}$ separated by a gate from the clear fluid. Then, the gate is removed and the particles flow due to gravity, without any constraint in the spanwise direction. We choose half of the box height as the characteristic length scale $h = L_2/2$. The velocity scale is defined by the buoyancy velocity as $u_b = \sqrt{g'h}$. The reduced gravitational acceleration g' is defined as $g' = g(\rho_p - \rho_0)c_i/\rho_0$ where ρ_p and ρ_0 are the particle and clear fluid density respectively, g is the gravitational acceleration and c_i is the initial volume fraction of the particles in the lock. With these two scales and the kinematic viscosity of the fluid ν, we can define the Reynolds number as $Re = u_b h/\nu$. All variables are made dimensionless using c_i, h or/and u_b.

Free-slip boundary conditions are imposed for the velocity field in the streamwise and spanwise directions x_1 and x_3 while no-slip boundary conditions are used in the vertical direction x_2. For the scalar field, no-flux conditions are used in the streamwise and spanwise directions x_1 and x_3, and in the vertical direction x_2 at the top of the domain. For the particles deposition in the vertical direction x_2 at the bottom of the domain, a simple 1D outflow boundary condition is imposed, meaning that the particles can virtually leave the computational domain (non conservative simulations). The modelling of the initial reservoir is performed with a customized immersed boundary method based on a direct forcing approach that ensures zero-velocity boundary conditions and a no-flux boundary condition for the fluid-particle mixture at the wall of the solid geometry. We solve the incompressible Navier-Stokes equations using the Boussinesq approximation along with a scalar transport equation on a Cartesian mesh with our high-order flow solver **Incompact3d** (www.incompact3d.com) which is based on sixth-order compact schemes for spatial discretization, a third order Adams-Bashforth scheme for time advancement and a fully spectral Poisson solver. Full details about the code can be found in [1].

---

*Corresponding author. Email: s.laizet@imperial.ac.uk

RESULTS

For this study, three simulations are performed with three different Reynolds numbers equal to 1000, 5000 and 10000. The computational domain $L_1 \times L_2 \times L_3 = 12 \times 2 \times 12$ is discretized with $1201 \times n_y \times 1201$ mesh points with n_y equal to 193, 289 and 385 for $Re = 1000$, 5000 and 10000 respectively. For the three simulations we use the same lock dimensions $L_{1s} \times L_{2s} \times L_{3s} = 1 \times 2 \times 2$ with a dimensionless settling velocity of $u_s = 0.02$ and a Schmidt number equal to 1. The formation, merging and meandering of the lobe-and-cleft structures at the front of the current can be seen in Figure 1. The observed slightly curved structures are different from the straight ones obtained with channelized or axisymmetric locks. For Re=1000, the structures are almost symmetric with respect to $x_3 = 0$ with very large lobe-and-left structures. When the Reynolds number is increased the structures become smaller and more curved. Note that the streamwise and spanwise extension of the current is the same for Re=5000 and Re=10000 suggesting a geometric similarity for the shape of the current for high Reynolds numbers.
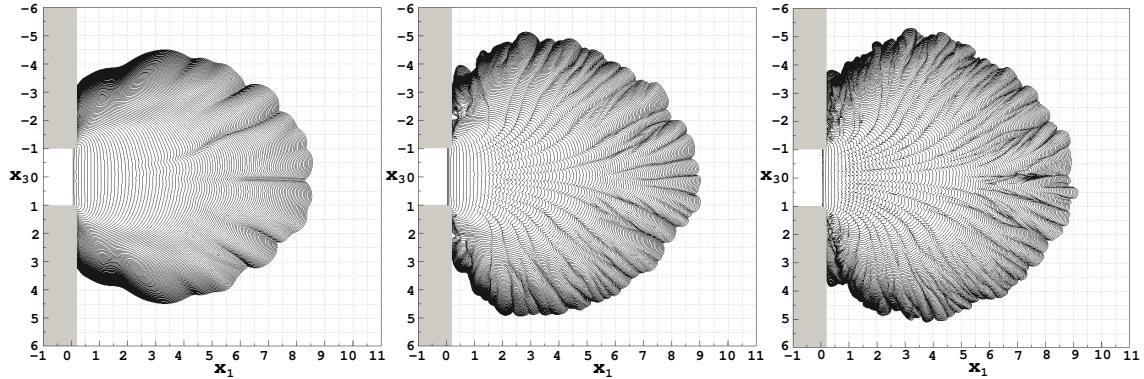

Figure 2: Time evolution of isolines of the bottom wall concentration for Re=1000 (left), 5000 (middle) and 10000 (right).

2D maps of the wall deposition $D_t(x_1, x_3, t) = \int_0^t c_w(x_1, x_3, \tau) u_s \, d\tau$ (where c_w is the concentration at the wall) are presented in Figure 3. As already explained for the channel configuration in a previous study [2], the lines starting from the initial volume and expanding with the current corresponds to the signature of the clefts. These maps can therefore be seen as a footprint of the front structures and can be used to better understand the lobe-and-cleft patterns. It can be seen that most of the deposition is location very close to the gate regardless of the Reynolds number. Once again, we can observe a very symmetric shape for the deposition at Re=1000 whereas at Re=10000 a large-scale bifurcation seems to split the deposit map in two large areas.
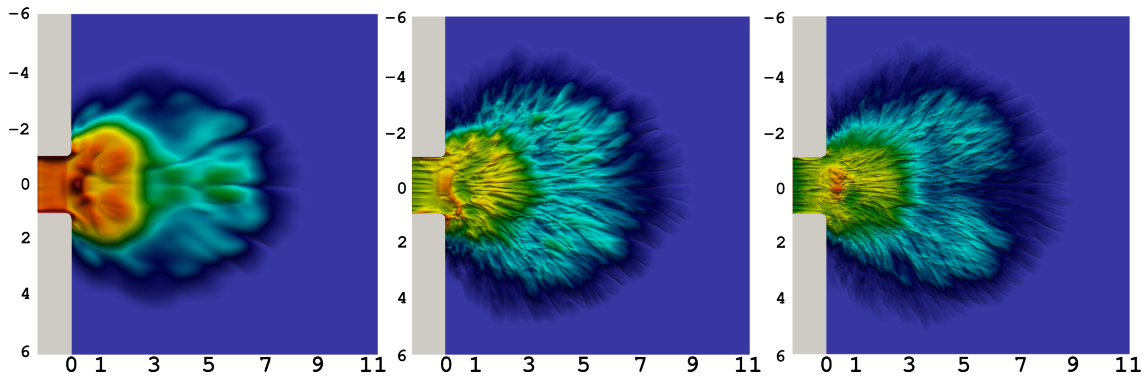

Figure 3: Deposit maps at $t = 20$ for Re=1000 (left), 5000 (middle) and 10000 (right). The data are normalized with the maximum values (red is 1, blue is 0).

References

[1] Laizet S. & Lamballais E.: High-order compact schemes for incompressible flows: a simple and efficient method with the quasi-spectral accuracy. J. Comp. Phys. 228: 5989-6015, 2009.

[2] Espath L.F., Pinto L.C., Laizet S. & Silvestrini J.H.: High-fidelity simulations of the lobe-and-cleft structures and the deposition map in particle-driven gravity currents. Physics of Fluids 27(5): 056604